2017

Magnetic Field Sensing Using Whispering Gallery Modes in a Cylindrical Microresonator Infilitrated With Ferronematic Liquid Crystal

Aseel Mahmood
Technological University Dublin

Vishnu Kavungal
Technological University Dublin, d12127257@mydit.ie

Sudad S. Ahmed
Baghdad University

Peter Kopcansky
Institute of Experimental Physics, Slovakia

Vlasta Zavisova
Institute of Experimental Physics, Slovakia

See next page for additional authors

Recommended Citation
Mahmood, A. et al. (2017). Magnetic field sensing using whispering-gallery modes in a cylindrical microresonator infiltrated with ferronematic liquid crystal. *Optics Express*, vol. 25, no. 11, pg. 12195-12202. doi:10.1364/OE.25.012195

Research Article | Vol. 25, No. 11 | 29 May 2017 | OPTICS EXPRESS 12195
Optics EXPRESS

Magnetic field sensing using whispering-gallery modes in a cylindrical microresonator infiltrated with ferronematic liquid crystal

ASEEL MAHMOOD,[1,2,*] VISHNU KAVUNGAL,[1] SUDAD S. AHMED,[2] PETER KOPCANSKY,[3] VLASTA ZAVISOVA,[3] GERALD FARRELL,[1] AND YULIYA SEMENOVA[1]

[1]*Photonics Research Centre, Dublin Institute of Technology, Kevin St., Dublin 8, Ireland*
[2]*Department of Physics, College of Science, Baghdad University, Iraq*
[3]*Institute of Experimental Physics SAS, Watsonova 47, 040 01 Košice, Slovakia*
[*]*aseelibrahim208@gmail.com*

Abstract: An all-fiber magnetic field sensor based on whispering-gallery modes (WGM) in a fiber micro-resonator infiltrated with ferronematic liquid crystal is proposed and experimentally demonstrated. The cylindrical microresonator is formed by a 1 cm-long section of a photonic crystal fiber infiltrated with ferronematic materials. Both ferronematics suspensions are prepared based on the nematic liquid crystal 1-(trans-4-Hexylcyclohexyl)-4-isothiocyanatobenzene (6CHBT) doped with rod-like magnetic particles in the first case and with spherical magnetic particles in the second case. WGMs are excited in the fiber microresonator by evanescent light coupling using a tapered fiber with a micron-size diameter. The Q-factor of the microresonator determined from the experimentaly measured transmission spectrum of the tapered fiber was 1.975×10^3. Under the influence of an applied magnetic field the WGM resonances experience spectral shift towards shorter wavelengths. The experimentally demonstrated sensitivity of the proposed sensor was −39.6 pm/mT and −37.3 pm/mT for samples infiltrated with rod like and spherical like ferromagnetic suspensions respectively for a magnetic field range (0-47) mT. Reducing the diameter of the cylindrical micro-resonator by tapering leads to enhancement of the magnetic field sensitivity up to −61.86 pm/mT and −49.88 pm/mT for samples infiltrated with rod like and spherical like ferromagnetic suspensions respectively for the magnetic field range (0-44.7) mT.

OCIS codes: (060.2310) Fiber optics; (060.2370) Fiber optics sensors; (060.4005) Microstructured fibers; (140.4780) Optical resonators; (160.3710) Liquid crystals.

References and links

1. A. Matsko and V. Ilchenko, "Optical resonators with whispering-gallery modes - Part I: Basics," IEEE J. Sel. Top. Quantum Electron. **12**(1), 3–14 (2006).
2. Y. Lu, J.-Q. Yao, P. Wang, and C.-Z. Zhang, "An investigation of a tapered fiber-microsphere coupling system with gain and evanescent-field sensing device," Optik (Stuttg.) **112**(10), 475–478 (2001).
3. D. Armani, B. Min, A. Martin, and K. Vahala, "Electrical thermooptic tuning of ultrahigh-Q microtoroid resonators," Appl. Phys. Lett. **85**(22), 5439–5441 (2004).
4. N. Pornsuwancharoen and P. P. Yupapin, "Entangled photon states recovery and cloning via the micro ring resonators and an add/drop multiplexer," Optik **121**(10), 897–902 (2009).
5. V. Zamora, A. Díez, M. V. Andrés, and B. Gimeno, "Cylindrical optical microcavities: Basic properties and sensor applications," Photonics Nanostruct. Fundam. Appl. **9**(2), 149–158 (2011).
6. A. Yalcin, K. Popat, J. Aldridge, T. Desai, J. Hryniewicz, N. Chbouki, B. E. Little, Oliver King, V. Van, Sai Chu, D. Gill, M. Anthes-Washburn, M. S. Unlu, and B. B. Goldberg, "Optical sensing of biomolecules using microring resonators," IEEE J. Sel. Top. Quantum Electron. **12**(1), 148–155 (2006).
7. J. Zhu, S. Ozdemir, Y. Xiao, L. Li, L. He, D. Chen, and L. Yang, "On-chip single nanoparticle detection and sizing by mode splitting in an ultrahigh-Q microresonator," Nat. Photonics **4**(1), 46–49 (2010).
8. V. Ilchenko and A. Matsko, "Optical resonators with whispering-gallery modes-part II: applications," IEEE J. Sel. Top. Quantum Electron. **12**(1), 15–32 (2006).
9. D. Zhu, Y. Zhou, X. Yu, P. Shum, and F. Luan, "Radially graded index whispering gallery mode resonator for penetration enhancement," Opt. Express **20**(24), 26285–26291 (2012).

#273803 https://doi.org/10.1364/OE.25.012195
Journal © 2017 Received 22 Aug 2016; revised 20 Nov 2016; accepted 24 Nov 2016; published 16 May 2017

Optics EXPRESS

10. S. Lane, F. Marsiglio, Y. Zhi, and A. Meldrum, "Refractometric sensitivity and thermal stabilization of fluorescent core microcapillary sensors: theory and experiment," Appl. Opt. **54**(6), 1331–1340 (2015).
11. M. Humar, M. Ravnik, S. Pajk, and I. Musevic, "Electrically tunable liquid crystal optical microresonators," Nat. Photonics **3**(10), 595–600 (2009).
12. Y. Liu, L. Shi, X. Xu, P. Zhao, Z. Wang, S. Pu, and X. Zhang, "All-optical tuning of a magnetic-fluid-filled optofluidic ring resonator," Lab Chip **14**(16), 3004–3010 (2014).
13. G. Brambilla, V. Finazzi, and D. Richardson, "Ultra-low-loss optical fiber nanotapers," Opt. Express **12**(10), 2258–2263 (2004).
14. P. Kopcansky, N. Tomasovicova, T. Toth-Katona, N. Eber, M. Timko, V. Zavisova, J. Majorosova, M. Rajnak, J. Jadzyn, and X. Chaud, "Increasing the magnetic sensitivity of liquid crystals by rod-like magnetic nanoparticles," Magnetohydrodynamics **49**(3–4), 586–591 (2013).

1. Introduction

Optical microresonators are axially symmetric structures that trap light in a small volume in the form of Whispering-Gallery Modes (WGMs). This effect occurs when light travels in a dielectric medium of circular geometry. After multiple repeated total internal reflections at the curved boundary, the electromagnetic field can close on itself and give rise to WGM resonances. Such microresonators have been investigated for applications in nonlinear optics, quantum electrodynamics, as optical filters, lasers and sensors for several decades [1]. But only recently have advances in micro- and nano-fabrication techniques made practical applications of micro resonators with physical dimensions in the order of optical wavelengths feasible. A wide range of optical resonators, such as microspheres [2], micro-disks [3], micro-rings [4] and cylindrical microcavities [5] have attracted significant interest from researchers worldwide. By using silica which is a highly transparent, low scattering loss material, WGM resonators with extremely high Q-factors and small mode volumes can be realised. Optical microresonators have shown many advantages in sensing applications due to their miniature size and high sensitivity allowing for low detection limits [6–8]. Many of the previously reported WGM sensors operate by detecting the shift in the resonant dips caused by the change of the refractive index (RI) of the medium surrounding the resonator due to the presence of chemical or biological materials on the resonator surface or in the surrounding solution [9, 10]. Several approaches proposed in the literature utilize liquid crystals or magnetic fluids to realise novel devices based on the WGMs. Humar et al. reported electrically tunable WGM resonators made of nematic liquid crystal droplets, embedded in a polymer matrix with the tunability of approximately two orders of magnitude larger than that achieved in solid-state microresonators [11]. Liu et al. infused a silica microcapillary-based ring resonator with a magnetic fluid, into which a laser pump light was injected by a fiber taper. Magnetic fluid strongly absorbes pump light which leads to a resonance shift of the silica microresonator due to the photothermal effect, resulting in tunning sensitivity of 0.15 nm/mW [12]. In this paper we report a novel magnetic field sensor utilizing WGMs in a cylindrical fiber microresonator infiltrated with a ferronematic LC. The sensor's structure and operating principle are as follows. A short section of a solid core photonic crystal fiber (PCF) acts as a cylindrical micro resonator in which the WGMs are excited by evanescent coupling of light propagating through a thin fiber taper placed perpendicularly and in direct contact with the PCF. The holes of the PCF are infiltrated with a ferronematic liquid crystal whose RI is sensitive to an applied magnetic field. Most WGM sensors reported in the literature are based on perturbation of the WGMs at the surface of the resonator, which in many cases leads to a poor stability of such resonators and often requires additional packaging of the resonator surface. In this work a ferronematic LC, which is key to sensing magnetic fields, lies within the body of the resonator, which leads to an improved stability. It has been found that lower order WGMs excited in such a micro resonator are strongly confined within the surface layer of the fiber resonator (in the outer cladding of the PCF), while the higher order modes expand further from the surface and into the body of the micro resonator [1].

Optics EXPRESS

2. Experimental details

The fiber used in our experiments is the commercially available Polarization Maintaining Photonic Crystal Fiber type PM-1550-01-PCF (Thorlabs). The fiber structure has five rings of air-holes around its asymmetric solid core. The small holes are ~2.2 μm in diameter and the inter-hole spacing is ~4.4 μm. The two large holes defining the birefringent axis of the fibre have a diameter of 4.5 μm. The outside diameter of the fiber is 122 μm an and the diameter of the holey region is 39.7 μm. Infiltration of the ferronematics liquid crystal in the 1 cm – long section of PM-PCF was carried out by dipping one end of the fiber into the ferronematic suspension so that the liquid infiltrated the PCF holes under the influence of capillary forces. The process was carried out at room temperature and pressure conditions. Two samples of ferronematic liquid crystal mixtures have been used in this work. Both ferronematics were based on the nematic liquid crystal 1-(trans-4-Hexylcyclohexyl)-4-isothiocyanatobenzene (6CHBT); which was doped with magnetic nanoparticles of different shapes: spherical and rod-like. Both magnetic suspensions consisted of Fe_3O_4 particles coated with oleic acid as a surfactant. The nematic-to-isotropic phase transition temperature (the clearing point) of the studied nematic was T_{NI} = 42.8 °C. The mean diameter of the spherical magnetic nanoparticles was 11.6 nm. The rod-like magnetic particles had a diameter of 80 nm, a mean length of 1200 nm and the volume concentration of the nanoparticles in both suspensions was 2×10^{-4}. Figure 1 TEM images for spherical and rod like ferronematic liquid crystal mixtures and optical microscope images of the PCF before and after infiltration [11], and SEM image of the PM-PCF cross section.

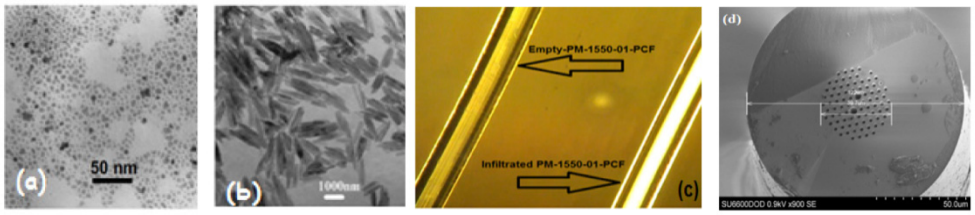

Fig. 1. TEM images of (a) spherical magnetic nanoparticles, (b) rod-like magnetic nanoparticles [16], (c) polarizing microscope images of empty and infiltrated PCF in crossed polarizers, and (d) SEM image of the PM-1550- 01-PCF cross section.

For the sensor interrogation, a fiber taper with a waist diameter of circa 1 μm was fabricated from a short length of a single mode fiber (SMF-28) using the customised microheater brushing technique [13]. The fiber tapering process was controlled by a customized computer program which realized a synchronized motion of two translation stages with fiber holders applying accurately calculated strain to the SMF. Figure 2 illustrates the experimental setup for the magnetic field sensor characterisation. A superluminescent diode (SLD) (Thorlabs) with a wavelength range of 1500-1600 nm is coupled to a polarization controller (DPC5500; Thorlabs) which in turn is coupled to the input end of tapered fibre, the output of which is coupled to an Optical Spectrum Analyzer (OSA) (Advantest, Q8384) with a wavelength resolution of 0.01 nm. The magnetic field was generated by a rectangular permanent magnet with dimensions of 2″x0.5″x 0.25″. The magnetic field strength was varied by changing the distance between the sensor fiber and the magnet as indicated by arrows in Fig. 2. A gauss meter probe (RS, GM08) was used as a reference to measure the magnetic field strength in the vicinity of the sensor fiber. One end of the PCF sensor fiber was fixed on the translation stage with an adjustable vertical position to allow for precise alignment perpendicularly and direct contact with the tapered fiber to achieve high coupling efficiency.

Optics EXPRESS

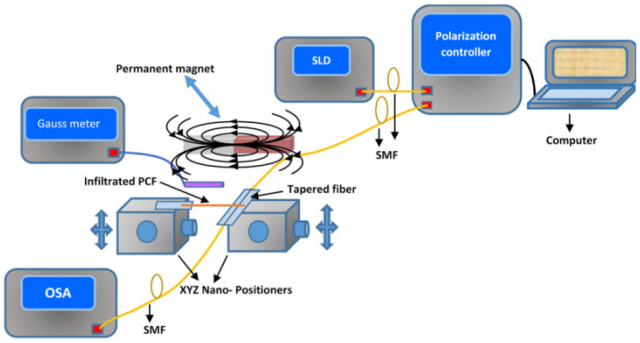

Fig. 2. Schematic diagram of the experimental setup for the magnetic field sensor characterization.

3. Results and discussion

Figures 3 (a) and 3(b) show the experimentally measured WGM transmission spectra and the Lorentzian fit used to estimate the Q-factor for the two sample resonators infiltrated with ferronematic LC containing rod-like and spherical particles respectively in the absence of magnetic field and at room temperature. As can be seen from the figures, the spectra contain periodic narrow dips corresponding to the WGM resonances. The Q-factor for the PCF samples infiltrated with ferronematic LC containing rod-like and spherical like particles are 1.975×10^3 and 1.628×10^3 respectively. The Q-factors are quite typical for this kind of cylindrical resonators, and their relatively low values are determined by strong scattering by the ferronematics and do not differ for the different kinds of nanoparticles.

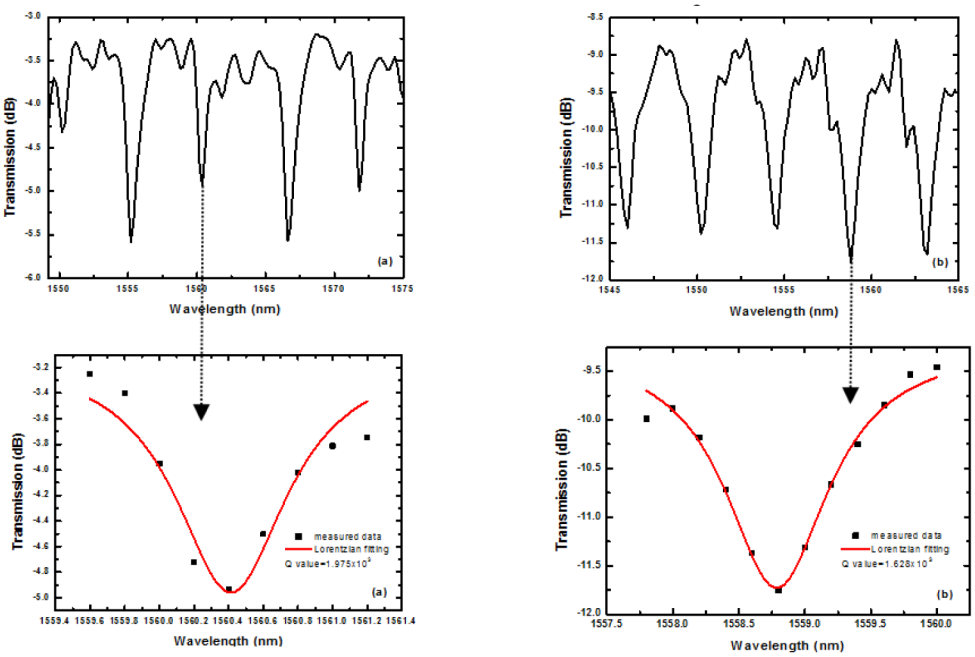

Fig. 3. Experimental WGM transmission spectra and corresponding Lorentzian fitting to estimate the Q-factor for the two sample resonators infiltrated with (a) rod-like, and (b) spherical particles containing ferronematic LC in the absence of magnetic field and at room temperature.

Optics EXPRESS

Following initial characterization both samples were subjected to varying magnetic fields by changing the distance between the permanent magnet and the sample, Figs. 4 (a) and 4(b) illustrate the changes in the WGM spectra for both samples under the influence of different values of the applied magnetic field. It can be seen that with an increase in the magnetic field strength, both spectra experience blue shifts and changes in the overall transmission loss level. The arrows in the figures indicate the direction of the spectral shift with the increase of the magnetic field strength. It should be noted that during the experiments changes in the spectral positions of the WGM resonances corresponding to the variations in the applied magnetic field were accurately tracked to eliminate the possibility of ambiguity in determining the wavelength shift direction. As expected, an increase in the applied magnetic field results in the changes of the effective refractive index of the ferronematic-filled fiber cladding, which via interaction with the evanescent field of the WGM leads to the observed blue-shift of the spectral positions of WGM resonances. The apparent increase in the transmission loss for both samples in Fig. 4 is likely due to the increased light scattering within the ferronematic LC since at higher values of the magnetic filed, greater portion of the WGMs volume overlaps with the ferronematic filled region of the microresonator.

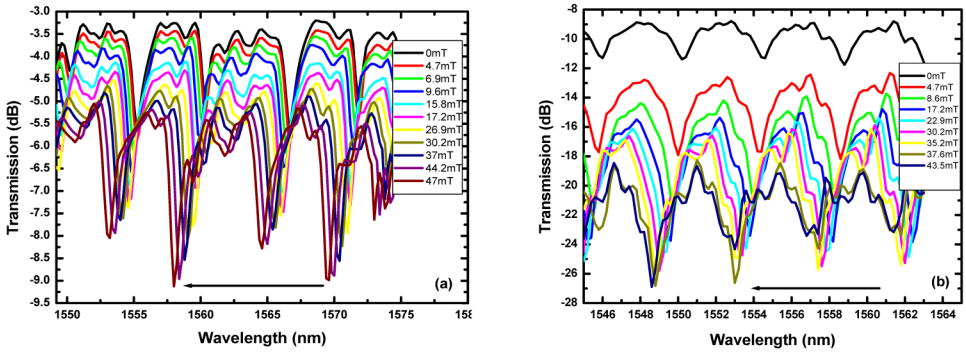

Fig. 4. (a) WGM spectra at different values of the applied magnetic field for the PM-1550-01-PCF infiltrated samples with (a) rod-like and (b) spherical particles.

Figures 5 (a) and 5(b) illustrates the dependencies of the two selected WGM resonances (at 1560.4 nm and 1558.8 nm for rod-like and spherical particles containing samples respectively) versus the applied magnetic field value. It can be seen that as the applied magnetic field strength increases the WGM resonant wavelengths decrease linearly at first, reaching saturation at values of the magnetic field above 50 mT and 45 mT for the rod-like and spherical samples respectively. The most likely reason for saturation is the complete re-alignment of all magnetic nanoparticles with the applied field, so that no further changes in the effective index of refraction occur as the magnetic field increases further.

Optics EXPRESS

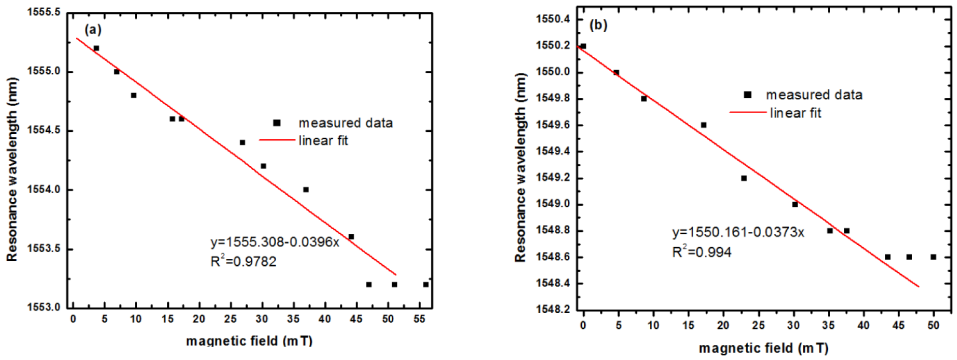

Fig. 5. Dependence of selected WGM resonant wavelengths and extinction ratio versus applied magnetic field: (a) rod-like particles containing sample and (b) spherical particles containing sample.

The maximum spectral shift values observed for each of the samples are –2 nm and –1.6 nm for the rod-like and spherical particles samples respectively. The corresponding average sensitivities of the sensor samples estimated from the experimental dependencies in Fig. 5 are circa –39.6 pm/mT and –37.3 pm/mT in the magnetic field range 0 - 50 mT. From the results we observed that the sensors where the PCF is infiltrated with a rod-like ferronematic liquid crystal sample are more sensitive to a magnetic field than those where the PCF is infiltrated with spherical like ferronematic liquid crystal sample. This is likely due to the dependence of the magnetic susceptibility on the nanoparticles morphology; doping with suspension containing particles with similar shape to the liquid crystal molecules (as in rod-like ferronematic liquid crystal) will result in lowering of the Fréedericksz transition threshold, as the applied field will more easily rotate the magnetic moments of the magnetic particles inside the ferronematic suspension. This realignment or rotation effect could then be extended to the host nematic through the coupling between the nanoparticles and the liquid crystal molecules. The realignment of the host nematic was assumed to be entirely determined by the ferromagnetic properties of the nanoparticles (not affected by the intrinsic diamagnetic properties of the nematic), since the theory of Brochard and de Gennes predicted a rigid anchoring with $\mathbf{n} \parallel \mathbf{m}$, where $\mathbf{n}$ is the unit vector of the preferred direction of the nematic molecules (director), and $\mathbf{m}$ is the unit vector of the magnetic moment of the magnetic particles [14]. Since the operating principle of the proposed sensor relies on the influence of the effective index of refraction in the PCF holey region on higher order WGMs excited in such a cylindrical resonator, it is reasonable to assume that decreasing the diameter of the PCF resonator could result in the increase of its sensitivity to the applied magnetic field. To verify this assumption we carried out an additional experiment for a similar sensor structure but in this case the PCF diameter was reduced down to 50 µm by tapering as shown in Fig. 6. The minimum diameter of 50 µm was chosen in order to prevent collapse of the air holes within the cladding.

Optics EXPRESS

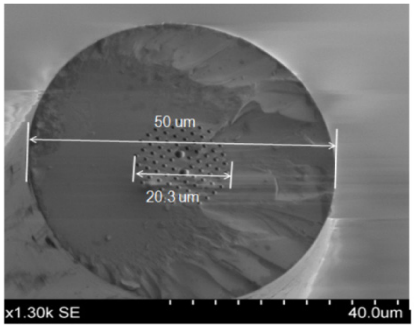

Fig. 6. The SEM image of the cross section of 50 μm tapered PM- 1550-01-PCFs.

Following the tapering the cylindrical resonators were infiltrated with the same ferronematic LC samples as in the previous experiments, Fig. 7 illustrates the selected WGM resonances as functions of the applied magnetic field. Analysis of the obtained results shows an increase in the sensitivity to −61.86 pm/mT for the sensor with the rod-like ferronematic LC and to −49.88 pm/mT for the spherical ferronematic LC sample respectively in the magnetic field range from 0 to 48.8 mT. It should be noted, that a small non-linearity of the resonant wavelength shift at low values of magnetic field for the rod-like sample (Fig. 7(a)) could be caused by a small reduction in the fiber cladding holes diameter due to tapering. This in turn may raise the value of the Fréedericksz transition threshold when the length of the rod-like particles becomes comparable with the diameter of cladding holes.

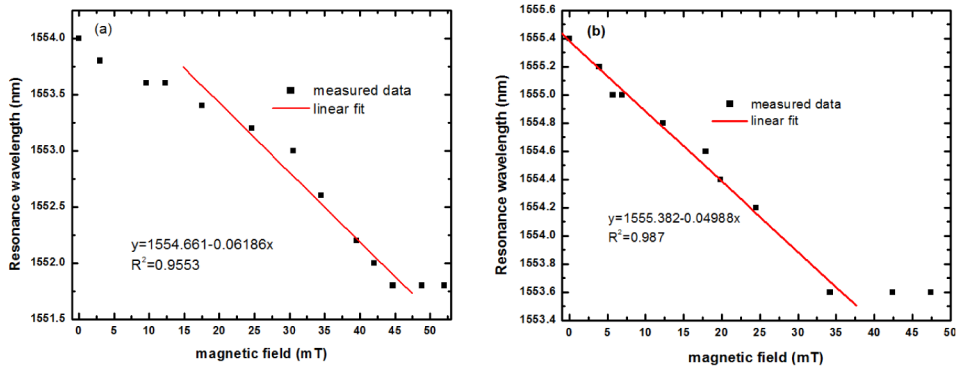

Fig. 7. Selected WGM resonance wavelength versus applied magnetic field for the tapered sensors (50 μm diameter): (a) rod-like particles sample and (b) spherical particles sample.

4. Conclusion

This paper reports a new type of a magnetic field sensor based on WGMs excited in a cylindrical micro resonator formed by a section of PM-01-1550-PCF infiltrated with a ferronematic LC. Perturbation of the RI of the magnetic fluid under the influence of the applied magnetic field results in the spectral shift of the WGM resonances detectable in the transmission spectrum of the tapered fiber positioned perpendicularly to the micro resonator. The experimentally demonstrated sensitivity of the proposed sensor is in the order of −39.6 pm/mT for the sensor infiltrated with the rod-like and −37.3 pm/mT for the spherical particles containing ferronematic LC respectively. Reducing the diameter of the cylindrical micro-resonator by tapering leads to enhancement of the magnetic field sensitivity up to −61.86 pm/mT for the sensor infiltrated with the rod-like and −49.88 pm/mT for the spherical particles containing ferronematic LC respectively.

Optics EXPRESS

Funding

This work was supported by projects VEGA 2/0045/13, MERANET MACOSYS, Ministry of Education Agency for Structural Funds of EU in frame of projects 6220120021 and 6220120033, and the Slovak Research and Development Agency under the contact No. APVV-015-0453.